Archives of Environmental Protection
Vol. 52 no. 2 pp. 53–66

PL ISSN 2083-4772
DOI: 10.24425/aep.2026.1294

Treatment of landfill leachate by an ultrasonic--three-dimensional electrode coupled reaction system

Xiaoyan Wei[1,2,*], Kang Li[1,2], Wanqi Wang[2,3], Tianhong Zhou[1], Jianjun Gao[4], Mingxia Jing[2], Shuaiqi Ren[2], Fulong Ye[2], Hao Wang[5]

[1]School of Environmental and Municipal Engineering, Lanzhou Jiaotong University, China
[2]College of Civil Engineering and Hydraulic Engineering
[3]School of Civil Engineering, Tianjin University, China
[4]Economic and Technological Development Bureau, Biotechnology Industrial Park Administrative Committee of Qinghai Province, China
[5]State Key Laboratory of Watershed Water Cycle Simulation and Regulation, China Institute of Water Resources and Hydropower Research, China

*Corresponding author's e-mails: Xiaoyan_Wei990022@126.com

Keywords: leachate, ultrasonic-three-dimensional electrode, coupled reaction system, synergistic index.

Abstract: Advanced oxidation technology has a excellent treatment effect on refractory wastewater. In this study, conventional, unmodified, and low-cost electrode materials were used to construct an ultrasonic three-dimensional electrode coupled reaction system (US-3DES), and its effectiveness in treating leachate from a closed municipal solid waste landfill was investigated. The results showed that, under the optimal treatment conditions, the COD and UV254 removal rates were 98.15% and 96.32%, respectively, after 120 min of reaction. This performance significantly surpassed that of single ultrasound (US) (COD and UV254 removal rates of 53.13% and 60.74%, respectively) and a single three-dimensional electrode system (3DES) (73.84% and 87.57%, respectively).Kinetic analysis showed that the reaction process exhibited the characteristics of a pseudo-first-order reaction in two stages. The calculated synergistic indices (SI_1 = 1.26, SI_2 = 9) demonstrated a significant synergistic effect in the coupled system. Free radicals in the coupled reaction system were detected by methylene blue spectrophotometry, and the results showed that hydroxyl radical concentration [•OH] reached up to 9.8×10-6 M. The steady-state free radical generation rates in the two kinetic stages were 9.7×10^{-9} M s^{-1} and 2.67×10^{-8} M s^{-1}, respectively. The energy consumption and treatment cost of US-3DES were 149.0 kWh•kg COD^{-1} and 25,021.1 CNY•kg COD^{-1}, respectively. This study confirms that US-3DES offers the following benefits: efficient leachate treatment, simple operation, low cost, and no requirement of additional chemicals. Additionally, it provides feasible solutions for the engineering applications of refractory wastewater treatment.

Introduction

Leachate originates from municipal landfills that receive solid waste, and the BOD/COD ratio of aged leachate (landfilled for more than10 years) is typically less than 0.1. Organic matter in leachate mainly comprises dissolved particles of solid waste and byproducts of biodegradation process in landfills. Owing to its complex composition and high recalcitrance, this wastewater poses significant treatment challenges.

Current approaches to landfill leachate treatment include biological, physical, and advanced oxidation processes (AOPs). Biological methods utilize microorganisms for direct oxidation treatment. Remmas et al. (2023) reported that leachate can effectively achieve biological denitrification in an anaerobic ammonium oxidation system. Xie et al. (2014) investigated landfill leachate treatment using an anaerobic dynamic membrane bioreactor and showed that the average COD removal efficiency reaches 62.2% under stable operating conditions. Research has also been conducted on enzymatic catalytic oxidation. Nalladiyil et al. (2023) used various biological enzymes to treat municipal landfill leachates. However, biological methods can only remove aliphatic, highly unsaturated, and phenolic substances from leachate, and high concentrations of refractory organic matter remain in the effluent after treatment. Physical methods mainly include coagulation–flocculation (Djeffal K, et al. 2021) and membrane-based processes (Bodzek M, 2019). However, these methods transfer pollutants from the liquid phase to the

solid phase without eliminating or degrading them. AOPs such as photocatalysis (Kanmani S, et al. 2023,Boonphan S, et al. 2024), Fenton/ozonation (Wu C, et al. 2021), wet air oxidation, and supercritical water oxidation (Parthenidis P, et al. 2022) primarily mineralize organic contaminants via radical generation and demonstrate potent oxidative capacity. However, compared to electrochemical oxidation and ultrasonication, these technologies either require chemical inputs or involve high capital and operational costs, which pose significant challenges for large-scale application.

Electrochemical oxidation removes pollutants by generating highly oxidizing free radicals on the electrode surface and mineralizing them into simple small-molecule compounds. This method has demonstrated excellent performance in treating various refractory organic pollutants, requires no additional chemicals, is easy to implement, and shows strong potential for large-scale applications. Compared to two-dimensional electrodes (2DES), three-dimensional electrodes (3DES) have a higher specific surface area, which can significantly enhance the mass-transfer coefficient. Zhu et al. (2011) reported that the removal rates of *p*-nitrophenol and COD using a three-dimensional electrode system were 2–7 times higher than those achieved with 2DES. However, 3DES often exhibit reduced degradation efficiency for organic pollutants owing to the uneven distribution of current and potential (Li H, et al. 2021). In addition, pollutants and their intermediate products may be adsorbed or deposited on the surface of particle electrodes, which weakens the ability of electrodes to capture and degrade pollutants, causing a decline in current efficiency (Li H, et al. 2021).

Ultrasound (US) is an advanced oxidation method that can conveniently and effectively generate hydroxyl radicals (·OH) (Bremner D, et al. 2011), and it can be applied to the destruction and adsorption of organic compounds (Yurchenko O I, et al. 2021). However, US alone exhibits low degradation efficiency. In one study, only a small amount of H_2O_2 was generated, and no ·OH was detected in the ultrasonic field, making it difficult to degrade nitrophenol using US alone (Zhu X, et al. 2011). Therefore, US is often combined with processes such as electrocoagulation, electro-Fenton, and electro-oxidation as an auxiliary technology to enhance the degradation efficiency of organic pollutants in refractory wastewater (Hassani A, et al. 2022). Testolin et al.(2021) investigated the use of US to enhance the chemical and biodegradation potential of Fenton and ozone processes for the treatment of crude oil-contaminated soil. The results indicated that US can increase the total organic carbon (TOC) removal rate. This enhancement is attributed to ultrasonic cavitation, which promotes the generation of Fe^{2+} (Hassani A, et al. 2025). Furthermore, US acts as a mixing agent in the reaction system, thereby improving mass transfer efficiency (Zhu X, et al. 2011).

Single treatment technologies are insufficient to meet discharge standards and achieve adequate toxicity reduction for landfill leachate (Hosseinikhah M, et al. 2025). To address this challenge, researchers have developed integrated processes that combine advanced oxidation processes (AOPs). For example, electrochemical oxidation can be coupled with Fenton's reagent to form the electro-Fenton (EF) process (Liu J, et al. 2025), thereby enhancing the degradation efficiency of refractory organic compounds. Babuponnusami et al. (20120 demonstrated that EF improves the oxidation of organic compounds . Chatraee et al, (2022) reported that Fe^{2+} is generated through the oxidation of iron anodes, while the Fe^{3+}/Fe^{2+} redox cycle is maintained under an applied electric field, which promotes the generation of ·OH from H_2O_2 (Chatraee M, et al. 2022). However, this technology exhibits excellent treatment performance at a pH range of 3–7. At pH > 7, $Fe(OH)_3$ precipitates and cannot participate in the catalytic cycle; at pH > 9, soluble $[Fe(OH)_4]^-$ species are produced, which lack the ability to catalytically decompose H_2O_2. The combination of ultrasonic technology with electrochemical oxidation can enhance mass transfer efficiency and activate the electrode surface, thereby accelerating the overall oxidation process. Dionisio et al. (2019) investigated the electrochemically coupled ultrasonic degradation of simulated wastewater containing methyl hydroxyformate, and found that the ultrasonic irradiation enhanced organic matter removal and accelerated total organic carbon oxidation. Similarly, Ai et al. (2010) reported that ultrasonic-assisted electrochemistry significantly enhances azo dye decolorization through a synergistic effect. However, previous studies have either relied on expensive electrode materials, such as boron-doped diamond (BDD), platinum, and titanium, or employed related technologies to further modify the materials. These approaches increase capital costs and may introduce risks of secondary environmental pollution.

Current research on electrochemical oxidation mainly follows three approaches. The first involves the use of expensive electrode materials, such as platinum, titanium, lead, and their oxides. Zhang et al. (2024) investigated the electrochemical conversion of ammonia using PbO_2-Ti mesh anode, a Ti mesh cathode, and granular activated carbon (GAC) as particle electrodes, achieving an ammonia conversion rate of 71.5% after 90 min. Sopaj et al. (2015) evaluated various anode materials, including carbon felt, carbon fiber, graphite, platinum, lead dioxide, dimensionally stable anodes (DSA), and boron-doped diamond (BDD), with stainless steel as the cathode. Their results showed that BDD, platinum, and carbon felt exhibited the highest oxidation ability, followed by graphite and carbon fiber, whereas DSA showed the lowest performance. Kuchtová et al. (2020) demonstrated that platinum and BDD electrodes, in the presence of chloride ions, can effectively decolorize and degrade the textile dye Acid Blue 80.

The second approach focuses on the fabrication or modification of electrode materials using electrochemical methods. Arjona et al. (2017) fabricated electrodes by electrodepositing Pb and Pt onto carbon-based substrates. Zambrano et al. (2020) studied the electrochemical degradation of phenol on platinum-coated titanium electrodes under different pH conditions, reporting complete degradation after 24 h under acidic conditions. . Zhang et al. (2020) prepared Ti-Si-Sn-Sb/GAC particle electrodes using the sol-gel method for the treatment of p-aminophenol (PAP) wastewater, achieving removal efficiencies of 89.45% for PAP and 75.17% for COD under optimal conditions.

The third approach involves the use of waste materials to promote electrode reuse. Yang et al. (2022) used graphite as the anode, stainless steel as the cathode, and steel slag as particle electrodes to treat simulated domestic wastewater, achieving nearly 100% ammonia nitrogen removal after 50 min of

electrolysis. However, electrode materials such as Pb, Pt, and BDD are significantly more expensive than graphite, ranging from tens to thousands of times higher in cost (Yang et al. 2022), which limits their large-scale application. In addition, electrode modification may introduce secondary environmental pollution, while the reuse of waste materials remains limited and may pose environmental risks. In contrast, carbon-based electrode materials are abundant, cost-effective, possess high specific surface area, and exhibit excellent electrical conductivity, making them highly suitable for electrochemical oxidation processes (Ma J et al. 2023).

In three-dimensional electrode treatment process, the degradation and mineralization efficiency of pollutants largely depends on the performance of particle electrodes. Activated carbon, owing to its high surface area and abundant oxygen-containing functional groups, demonstrates excellent adsorption and electro-adsorption capacities (Sopaj, Flamur et al. 2015). Moreover, a synergistic effect exists between 3DES and activated carbon. Under an electric field, activated carbon becomes polarized, generating electroactive sites. Pollutants can be directly oxidized at the electrode surface or adsorbed onto activated carbon, where they are subsequently degraded by reactive species, enabling in situ regeneration of the adsorbent. This synergistic mechanism enhances both pollutant removal efficiency and the service life of activated carbon (Zhu X, et al. 2011).

Hydroxyl radicals (OH) are regarded as the primary reactive species in the oxidation of organic pollutants and play a key role in dye degradation. Common detection techniques for free radicals, such as electron spin resonance (ESR) spectroscopy and high-performance liquid chromatography (HPLC), offer high precision. However, these methods require expensive instrumentation , involve high operational and maintenance costs, and necessitate complex sample pretreatment, which limits their practical applicability. In contrast, spectrophotometric methods employ simple instrumentation, are easy to operate, incur low costs, and require minimal sample pretreatment, making them more widely applicable.

The aqueous solution of MB reacts with ·OH to form the reduced species OH- and MB radical cations. Because MB dye is dark blue whereas MB radical cations are colorless, the addition of a sample containing hydroxyl radicals to MB solution causes the color to change from dark blue to colorless (Satoh A Y, et al. 2007). The reaction is shown in Equation (1):

$$MB + \cdot OH \rightarrow MB^{2+\bullet} + HO^{-} \quad (1)$$

Using MB as the capture agent, a spectrophotometric method has been applied to determine hydroxyl radicals (Chen, Wang, et al. 2018). This simple, low-cost detection method provides an effective alternative to complex instrumentation and can enhance the research capabilities of laboratories with limited resources (Lankone R S, et al. 2020, Erel O, 2004).

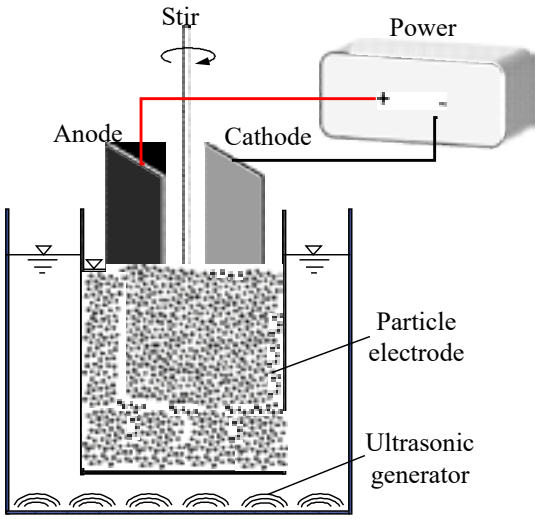

Fig. 1. Experimental setup

This study examined leachate from a closed municipal solid waste landfill. Conventional, unmodified, low-cost electrode materials (graphite, stainless steel, and activated carbon) were used to construct a US-3DES. A spectrophotometric method was adopted to determine ·OH in the reaction system, and the treatment efficacy of this system for landfill leachate was further explored, thereby providing a basis for future engineering applications of this technology.

Materials and methods

Instruments and reagents

Analytical-grade sodium sulfate, mercuric sulfate, silver sulfate, and potassium dichromate were used. An ultraviolet (UV)-visible spectrophotometer (TU-1810, Beijing Puxi General Instrument Co., Ltd., Beijing, China) was used for free radical detection.

Experimental setup

The experimental setup (shown in Figure 1) consisted of an adjustable DC-regulated power supply (APS3005D, Nanjing Guorui Antaixin Technology Co., Ltd., Nanjing, China), a reactor (100 × 100 × 140 mm plexiglass), and electrodes (graphite as the anode, purchased from Qingdao Baofeng Graphite Products Co., Ltd., Shandong, China, stainless steel as the cathode, commercially available, both with dimensions of 100 × 100 × 5 mm). It also included a particle electrode [powdered activated carbon (PAC), purchased from Gongyi Baiqing Chemical Industry Co., Ltd., Henan, China, with a specific surface area of 1100 $m^2 \cdot g^{-1}$ and a

Table 1: Table 1 The quality of leachate

Water quality indicators	Value	Waterquality indicators	Value
pH	7.8~8.9	Conductivity / $ms \cdot cm^{-1}$	29.3~43.4
COD / $mg \cdot L^{-1}$	1850~4462	UV_{245} / $AU \cdot cm^{-1}$	21.23~28.65
BOD / $mg \cdot L^{-1}$	516~875	Salinity / $g \cdot L^{-1}$	17.87~25.25
NH_3-N / $mg \cdot L^{-1}$	1420~2879	Fe^{2+} / $mg \cdot L^{-1}$	0.079~0.265
TOC / $mg \cdot L^{-1}$	3987	Total Iron / $mg \cdot L^{-1}$	0.117~0.392

pore size predominantly distributed in the range of 10–50 nm; and the PAC was subjected to saturated adsorption with landfill leachate prior to the experiments], an ultrasonic generator (JP-120ST, Jiemeng Ultrasonic Technology Co., Ltd., Shenzhen, China), and a mechanical stirrer (JJ-1A 60 W, Xicheng Xinrui Instrument Factory, Jintan District, Changzhou, China).

Experimental water sample

The leachate used in the experiment was collected from a municipal solid waste landfill in Xining City, Qinghai Province, China, which began operation in 1999 and ceased operation in 2020. Sampling was conducted every 2–3 weeks. After filtration, the samples were sealed in plastic bottles and stored in a refrigerator at 4 ℃ until analysis. The characteristics of the landfill leachate are presented in Table 1.

Evaluation method

Leachate (1 L) was added to the reactor, and sodium sulfate (6 g) was introduced as the electrolyte. Single-factor experiments were conducted to investigate four parameters: particle electrode weight (40–80 g), electrode spacing (4–6 cm), current density (20–60 $mA \cdot cm^{-2}$), and applied voltage (10–20 V). These variables were evaluated based on their effects on COD and UV_{254} removal to identify the optimal 3DES operating conditions. Under these optimized conditions, ultrasound power (0–600 W) was further examined to determine the optimal degradation parameters for the integrated US-3DES. All experiments were conducted for 120 min, with sampling at 30 min intervals.

Removal rate

COD was determined using the fast digestion spectrophotometric method (HJ/T 399-2007). Leachate characterization was performed at λ = 254 nm using a UV-vis spectrophotometer (TU-1810). The removal rates were calculated using Equation (2):

$$\text{Removal rate}(\%) = \frac{(C_0 - C_i)}{C_0} \cdot 100\% \quad (2)$$

where C_0 and C_i are the initial and final concentrations of COD ($mg \cdot L^{-1}$) and UV_{245} ($AU \cdot cm^{-1}$), respectively.

Synergistic index (SI)

The synergistic index (SI) was evaluated using the kinetic rate constants of different reaction systems (3DES, US, and US-3DES) to verify the effectiveness of the coupling process. The SI was calculated according to Equation (3) (Dionisio D, et al. 2019) :

$$SI = \frac{k_{US-3DES}}{k_{US} + k_{3DES}} \quad (3)$$

where k_{3DES}, k_{US}, and $k_{US\text{-}3DES}$ are the apparent kinetic rate constants for the individual and coupled processes, respectively. An SI > 1 indicates a synergistic effect, reflecting enhanced performance of the coupled process; the larger the SI value, the stronger the synergistic effect. An SI = 1 indicates an additive effect, meaning that the coupled process provides no additional synergistic benefit. An SI < 1 indicates an antagonistic effect, suggesting that the coupled process has an detrimental impact (Yang H, et al. 2021).

Determination of free radicals

An aqueous MB solution with a concentration of 0.025 $mmol \cdot L^{-1}$ was prepared. The solution was treated using the US-3DES reaction system under optimized conditions, and samples were collected at 0, 30, 60, 90 and 120 min of the reaction. The absorbance of the samples was measured at λ = 664 nm using an ultraviolet-visible spectrophotometer. During the experiment, OH radicals were continuously generated in the reaction system, therefore a pseudo-first-order kinetic model was established (Abbas S M, et al.,2025).

$$-\frac{d[MB]}{dt} = K_{app}[MB] \quad (4)$$

Where K_{app} is the apparent rate constant (min^{-1}). Through integration, the rate law for the pseudo-first-order reaction can be rearranged as follows:

$$\ln[MB]_t = \ln[MB]_0 - K_{app} t \quad (5)$$

Where $[MB]_0$ and $[MB]_t$ represent the initial concentration and the concentration at time t ($mg \cdot L^{-1}$), respectively. These concentrations can be expressed in terms of the initial absorbance (A_0) and the absorbance at time t (A_t). Equation (5) can thus be rearranged as follows:

$$\ln\frac{A_t}{A_0} = -k_{app} t \quad (6)$$

Where k_{app} can be determined from the slope of the linear plot obtained by plotting $\ln\left(\frac{A_t}{A_0}\right)$ as a function of time. According to the Beer-Lambert law, the following relationship holds:

$$\Delta[MB] = \frac{(A_0 - A_t)}{\mu L} \quad (7)$$

Where △[MB] represents the change in the concentration of MB from 0 to t (M). Based on Equation (3) and the reaction stoichiometric ratio, the following expression can be derived:

$$[\cdot OH] = \frac{\Delta[MB]}{\eta} \quad (8)$$

Where η represents the reaction stoichiometric ratio. The primary method used in this study was to calculate the free radical concentration by monitoring the decolorization of MB using an ultraviolet-visible spectrophotometer. Hydroxyl radicals (·OH) induce decolorization by breaking the conjugated structure of MB through addition reactions, requiring 1–2 M of ·OH. Therefore, the stoichiometric ratio was set to 2 in this study. The steady-state generation rate of hydroxyl radicals (R_{OH}, $M\ s^{-1}$) is expressed as:

$$R_{OH} = k_{app}\frac{[MB]_0}{\eta} \quad (9)$$

Energy consumption and treatment cost calculation

Electric energy consumption (EC) is a key component of the operational costs of electricity-based advanced oxidation processes (EAOPs), such as ultrasonic and electrochemical oxidation. In this study, EC_{3DES} and $EC_{US\text{-}3DES}$ were calculated using Equations (10) and (11), respectively.

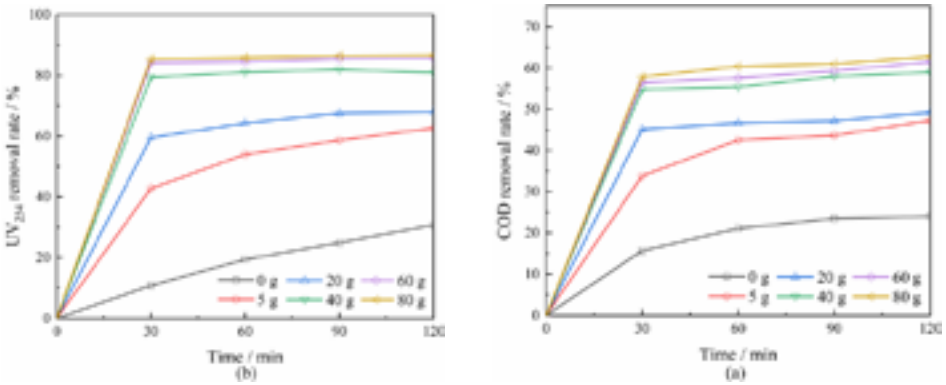

Fig. 2. Effect of PAC dosage on the removal rate of: (a) chemical oxygen demand (COD); (b) UV_{254}.

$$EC_{3DES}\left(kWh\cdot kg\,COD\right)=\frac{I\,U\,\Delta t}{1000\;\Delta COD\,V} \qquad (10)$$

$$EC_{US-3DES}\left(kWh\cdot kg\,COD\right)=\frac{\left[I\,U+P\right]\Delta t}{1000\;\Delta COD\,V} \qquad (11)$$

Where I is the current (A), U is the voltage (V), P is the ultrasonic power (W), Δt is the reaction time (h), $\triangle$COD denotes the experimental COD decay in solution (kg·m^{-3}), and V is the volume of the solution (m^3).

In this study, the treatment cost (TC) was calculated using Equation (12).

$$\mathrm{TC}\left(\mathrm{CNY}\cdot\mathrm{kg\ COD^{-1}}\right)=\frac{\mathrm{C}}{\Delta\mathrm{COD}} \qquad (12)$$

Where C represents the treatment cost, including the costs of materials, equipment and electricity (CNY).

Results and discussion

Optimal conditions for the 3DES

Effect of activated carbon dosage on removal rate

Adding an appropriate amount of saturated PAC to the 2DES to construct a 3DES not only enhances mass-transfer efficiency but also promotes organic matter degradation (Cho S, et al. 2020). Under conditions of an electrode spacing of 6 cm , a current density of 40 mA·cm^{-2}, and an initial voltage of 15 V, the effects of different activated carbon dosages on the leachate removal rate were investigated. The experimental results are presented in Figure 2.

As shown in Figure 2, the removal rate increased with increasing activated carbon dosage. At an activated carbon dosage of 80 g and reaction time of 120 min, the COD and UV_{254} removal rates reached their highest values, at 62.8% and 86.7%, respectively. The removal performance of the 3DES was significantly higher than that of 2DES. When the activated carbon dosage was 0, the system could be regarded as a 2DES, for which the maximum COD and UV_{254} removal rates were only 24.0% and 30.7%, respectively. This improvement can be attributed to the role of activated carbon in the 3DES. As a particle electrode, it not only reduced mass-transfer resistance in the reaction process (Shi H, et al. 2020) but also facilitated the formation of ·OH in the reaction system. This enhanced indirect oxidation reactions [Equations (13) and (14)] (Zhang C, et al. 2013), while direct oxidation of leachate also occurred at the electrode surface [Equation (15)] (Cho S, et al. 2020).

$$2H_2O \rightarrow 2\cdot OH + 2H^+ + 2e^- \qquad (13)$$

$$\mathrm{Leachate} + \cdot OH \rightarrow \mathrm{oxidized\ products} + H_2O \qquad (14)$$

$$\mathrm{Leachate} \xrightarrow{\text{particle electrode surface}} e^- + \\ +H_2O+\mathrm{oxidized\ products} \qquad (15)$$

Increasing the number of particle electrodes increases the number of polarized microelectrodes, thereby expanding the effective electrode reaction area for pollutant degradation. This promotes the formation of highly oxidizing substances at active sites and reduces the mass transfer distance between pollutants and free radicals, improving removal efficiency (Sopaj Flamur,

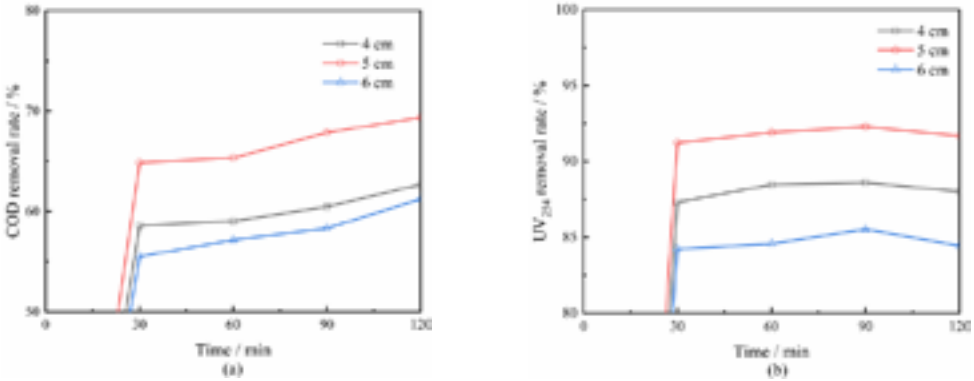

Fig. 3. Effect of electrode spacing on removal rate of: (a) chemical oxygen demand (COD); (b) UV_{254}.

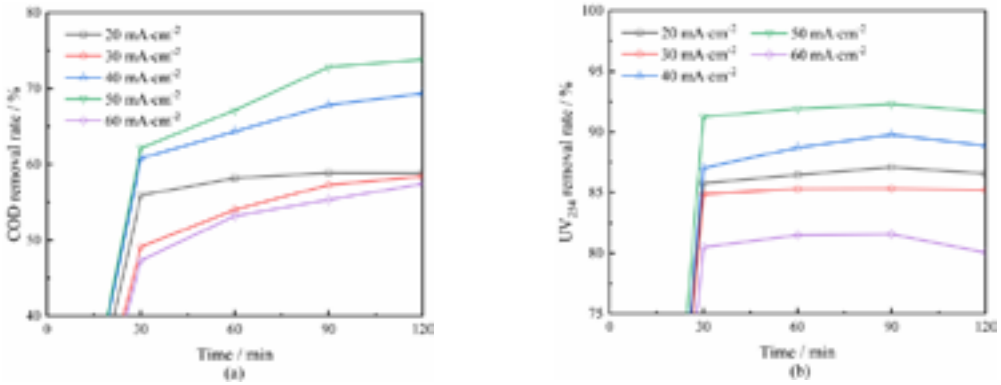

Fig. 4. Effect of current density on removal rate of: (a) chemical oxygen demand (COD); (b) UV_{254}.

et al. 2015). However, when the activated carbon dosage was 60 g and the reaction time was 120 min, the COD and UV_{254} removal rates were 61.5% and 85.6%, respectively, with only minimal differences from the removal rates observed at 80 g. Although adding particle electrodes effectively increases the reaction area in the reactor, excessive concentrations provide little additional benefit (Yu D, et al. 2020). This is because a large number of particle electrodes frequently collide in the reactor, causing short circuits in the 3DES (Ren X, et al. 2024). Therefore, 60 g of activated carbon was selected as the optimal reaction condition in this study.

Effect of electrode spacing on removal rate

The distance between the electrodes determines their degree of polarization (Shen B, et al. 2017). Under conditions of an activated carbon dosage of 60 g, current density of 40 mA·cm^2, and a preset voltage of 15 V, the effect of different plate spacings on the leachate removal rate was investigated. The experimental results are presented in Figure 3.

As shown in Figure 3, the removal rate decreased when the electrode spacing was either excessively small or large. At a plate spacing of 5 cm, the COD and UV_{254} removal rates reached their maximum values of 69.4% and 91.7%, respectively. Both smaller and larger electrode spacings resulted in lower removal efficiencies, with the lowest removal rate observed at a spacing of 6 cm. A smaller electrode spacing promotes passivation of the electrode surface (Shen B, et al. 2017). In contrast, when the spacing is too large, many particle electrodes remain unpolarized outside the electric field between the two electrodes, weakening their polarization effect (Huang Z, et al. 2024) and reducing the oxidation capacity of the system. As the electrode spacing increases, these previously unpolarized particle electrodes enter the inter-electrode region and become polarized, increasing the number of active electrodes and enhancing pollutant removal (Zhao H, et al. 2015). In addition, increasing the electrode spacing improves solution mixing and reduces concentration polarization near the electrode surfaces (Zambrano J, et al. 2020). However, further increases in spacing lead to a decline in removal performance. This is attributed to increased mass transfer resistance within the reactor (Kishore K, et al. 1989), a larger voltage drop between electrodes, and a decrease in current density (Zhao H, et al. 2015), all of which reduce the reaction rate. Therefore, an electrode spacing of 5 cm electrode was selected as the optimal condition in this study.

Effect of current density on removal rate

The current density is an important factor controlling the electrochemical reaction rate on the electrode surface (Hassani A, et al. 2022). Under conditions of an activated carbon dosage of 60 g, an electrode spacing of 5 cm, and a preset voltage of 15 V, the effects of different current densities on the leachate removal rate were investigated. The experimental results are presented in Figure 4.

As shown in Figure 4, the removal rate increased with increasing current density. At a current density of 50 mA·cm^{-2} and a reaction time of 90 min, the COD and UV_{254} removal rates reached their highest values of 73.8% and 91.7%, respectively. This is because the increase in current density promoted ·OH formation, thereby accelerating organic pollutant mineralization (Periyasamy S, et al. 2022). However, an excessively high current density can decrease the removal rate. For example, when the current density was 60 mA·cm^{-2}, the COD and UV_{254} removal rates significantly decreased to 57.45% and 80.06%, respectively. This was mainly because, at excessively high current densities, side reactions such as hydrogen evolution [Equation (16)] and oxygen evolution [Equations (17) and (18)] increased in the reaction system, competing with organic matter oxidation (Li H, et al. 2021). A large number of bubbles formed on the electrode surface, preventing organic matter from coming into contact with the electrode surface (Yu D, et al. 2020) and reducing effective mass transfer at the anode surface. This affects direct oxidation, thereby reducing the removal rates. Additionally, excessively high current density is more likely to cause electrode corrosion and increase the EC of the reaction system (Zhao H, et al. 2015). When the current density is too low, the number of free radicals produced is low, and electrochemical oxidation is constrained by mass transfer (He, et al. 2018), resulting in poor degradation. Therefore, 50 mA·cm^{-2} was adopted as the optimal reaction condition in the this study.

$$2H^+ + 2e^- \rightarrow H_2 \tag{16}$$

$$4OH^- \rightarrow O_2 + 2H_2O + 4e^- \tag{17}$$

$$H_2O \rightarrow \frac{1}{2}O_2 + 2H^+ + 2e^- \tag{18}$$

Effect of preliminary set voltage on removal rate

Voltage has a significant effect on electrochemical degradation efficiency (Li M, et al. 2015). The effects of

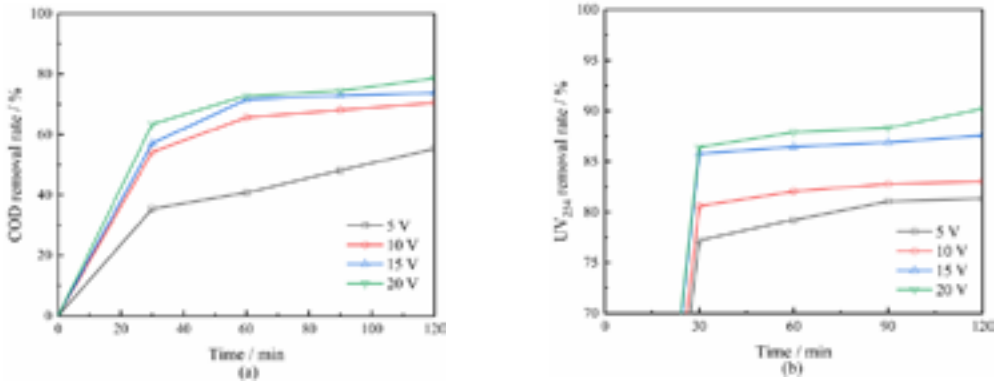

Fig. 5. Effect of preliminary set voltage on the removal rate of: (a) chemical oxygen demand (COD); (b) UV_{254}.

different preset voltages on the leachate removal rate were investigated under the conditions of an activated carbon dosage of 60 g, electrode spacing of 5 cm, and a current density of 50 $mA \cdot cm^{-2}$. The experimental results are presented in Figure 5.

As shown in Figure 5, under a constant current density, the removal rate increased with increasing preset voltage. At 20 V and a reaction time of 120 min, the COD and UV_{254} removal rates reached their maximum values of 78.6% and 90.21%, respectively. This is because, as the preset voltage increased, the oxidation capacity of the electrode surface also increased, thereby improving the direct oxidation capacity of the electrode (Ren X, et al. 2024). Moreover, the increase in preset voltage intensified the polarization of the particle electrode (Zhao H, et al. 2015), which promoted ·OH generation and enhanced the indirect oxidation capacity of the reaction system. However, when the preset voltage increased from 15 V to 20 V, the improvement in removal rate diminished. This may be attributed to the intensification of competing side reactions at higher voltages, as well as an increase in EC with increasing voltage (Yao Y, et al. 2020). In addition, as the electrolysis voltage continues to rise, part of the applied voltage does not contribute to electrode reactions but instead dissipates in the electrolyte, reducing the effective potential difference between the electrolyte and the electrodes. This, in turn, slows both direct and indirect oxidation reactions of pollutants and lowers electrolysis efficiency (Zambrano J, et al. 2020). Furthermore, a large number of gas bubbles generated at higher voltages adhere to the electrode surface, hindering direct oxidation reactions (Zambrano J, et al. 2020). Therefore, 15 V was selected as the optimal experimental voltage in this study, under which the removal rates of COD and UV_{254} were 73.84% and 87.57%, respectively, at a reaction time of 120 min.

Selection of optimal ultrasound conditions for the 3DES

Ultrasonic frequency is an important parameter affecting the efficiency of ultrasonic electrochemical treatment (Hassani A, et al. 2022). In this study, an ultrasonic cleaner was used as the ultrasonic generator. The instrument had a rated frequency of 28 kHz and its power range was 0–600 W, with only power adjustment available. Therefore, under 3DES conditions, an activated carbon dosage of 60 g, electrode spacing of 5 cm, current density of 50 $mA \cdot cm^{-2}$, and a preset voltage of 15 V, the effects of different ultrasonic power levels on the leachate removal rate in the coupled reaction system were investigated. The experimental results are presented in Figure 6.

As shown in Figure 6, under constant ultrasonic frequency, the removal rate increased with increasing ultrasonic power. At 600 W, the COD and UV_{254} removal rates reached their maximum values of 95.6% and 99.01%, respectively, with a particularly notable increase in UV_{254} removal. After 30 min, the lowest removal rate observed was 90.34%. This trend can be attributed to the fact that higher ultrasonic power leads to greater cavitation intensity and faster reaction rates (Yao Y, et al. 2020). Ultrasonic waves produce cavitation effects, whereby their propagation in liquids occurs through molecular vibration in the medium, generating alternating expansion and compression cycles. As the pressure decreases, water rapidly transitions from liquid to gas, forming bubbles that collapse with significant implosion forces.

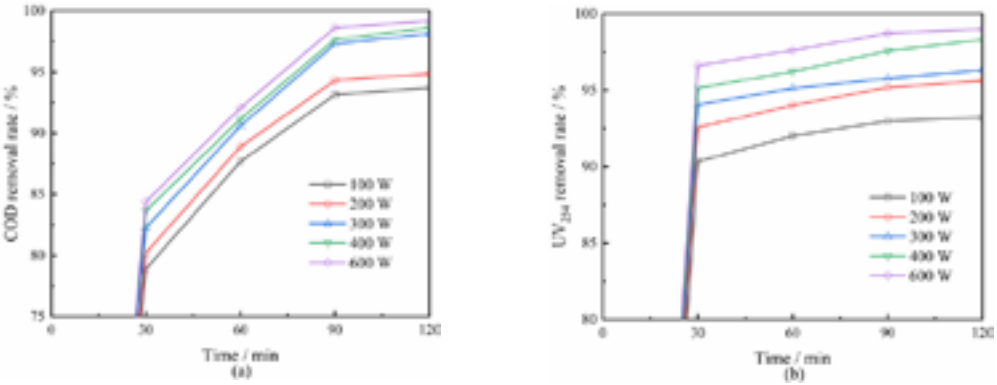

Fig. 6. Effect of ultrasonic power on the removal rate of: (a) chemical oxygen demand (COD); (b) UV_{254}.

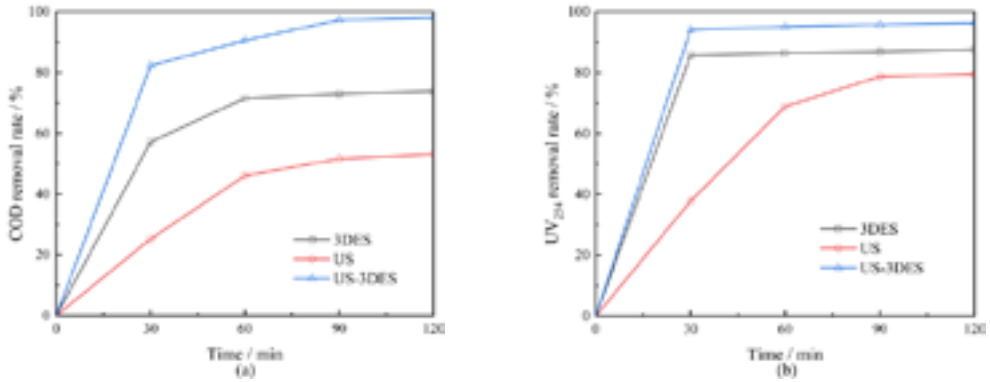

Fig. 7. Effect of three different treatment methods on removal rate of: chemical oxygen demand (COD); (b) UV_{254}.

These bubbles grow and collapse under the action of ultrasonic waves (Moholkar V S, et al. 2000).

The temperature and pressure inside collapsing bubbles can reach 4726.8 ℃ and 9869 atm, respectively (Moholkar V S, et al. 2000), leading to the decomposition of water molecules into highly oxidative radicals, as shown in Equations (19) – (28) (Hassani A, et al. 2022, Dionisio D, et al. 2019).

Owing to the rapid increase in pressure and temperature within the bubbles, hydrophobic substances are degraded when they approach or enter the collapsing bubbles due to bond cleavage. If these substances penetrate the interior of a cavitation bubble, the concentrated energy inside the bubble can effectively decompose them (Moholkar V S, et al. 2000). Hydrophilic substances are mainly degraded during cavitation in two regions: within the bulk liquid and at the gas–liquid interface of collapsing bubbles. In the bulk liquid, degeneration occurs primarily through reactions with free radicals, whereas at the gas–liquid interface, it is mainly driven by thermal decomposition (Moholkar V S, et al. 2000).

In addition, free radicals generated by ultrasonic cavitation exhibit an excellent decolorization effect (Dionisio D, et al. 2019). However, higher ultrasonic power also results in increased noise. Moreover, compared with 300 W, the COD removal rate at 600 W increased by 13.5%, whereas the UV_{254} removal rate increased by only 1.2%. Therefore, 300W was selected as the optimal operating power in this study.

$$H_2O \xrightarrow{\text{Ultrasound}} H\cdot + \cdot OH \quad (19)$$

$$H_2O + H\cdot \rightarrow \cdot OH + H_2 \quad (20)$$

$$O_2 + H\cdot \rightarrow HO_2^{\bullet} \quad (21)$$

$$2HO_2^{\bullet} \rightarrow H_2O_2 + O_2 \quad (22)$$

$$HO_2^{\bullet} + \cdot OH \rightarrow H_2O_2 + O_2 \quad (23)$$

$$H\cdot + O_2 \rightarrow \cdot OH + O\cdot \quad (24)$$

$$2\cdot OH \rightarrow H_2O_2 \quad (25)$$

$$H_2O_2 \xrightarrow{\text{Ultrasound}} 2\cdot OH \quad (26)$$

$$\cdot OH + HO_2^{\bullet} \rightarrow H_2O + O_2 \quad (27)$$

$$H_2O_2 + H\cdot \rightarrow H_2O + \cdot OH \quad (28)$$

Effect of different treatment methods on the removal rate

To evaluate the removal efficiency of the ultrasonic-three-dimensional electrode coupled system for leachate treatment, experiments were conducted under the following conditions: an activated carbon dosage of 60 g, electrode spacing of 5 cm, current density of 50 $mA \cdot cm^{-2}$, preset voltage of 15 V, and ultrasonic power of 300 W. The leachate was treated using three reaction systems: 3DES, US, and US-3DES. The results are presented in Figure 7.

The removal rates of the three reaction systems reached their maximum values after 120 min (Figure 7). Among them, the US treatment exhibited the lowest treatment efficiency, with maximum COD and UV_{254} removal rates of 53.1% and 79.5%, respectively, followed by the 3DES systems (73.8% and 87.6%, respectively). The US-3DES system showed the best performance, achieving maximum removal rates of 82.2% for COD and 96.3% for UV_{254} . This enhanced performance can be attributed to the application of ultrasonic waves during the electrochemical process, which generate acoustic streaming, leading to local turbulence and microcirculation in the fluid and thereby significantly reducing mass-transfer resistance (Moholkar V S, et al. 2000). During this process, free radicals generated at the electrode surface rapidly diffuse into the bulk solution, increasing their concentration and enhancing pollutant degradation efficiency (Moholkar V S, et al. 2000). These results indicate a positive synergistic effect between the ultrasonic irradiation and electrochemical oxidation (Ai Z, et al. 2010).

Kinetics analysis [Figure 8(a)] showed that all three systems followed two quasi-first-order reaction stages. The first stage (0-60 min) corresponded to a rapid reaction phase, with apparent rate constants of 0.021 min^{-1}, 0.010 min^{-1}, and 0.039 min^{-1} for3DES, US, and US-3DES, respectively. This behavior is mainly attributed to the rapid generation of ·OH radicals and the availability of abundant active sites on the electrode surface. The rate constant of the coupled system was 1.86 times and 3.9 times higher than those of the individual systems, indicating significantly enhanced free radical generation efficiency. During this stage, readily degradable organic compounds in the leachate were rapidly oxidized, resulting in a substantial increase in COD removal rate.

The second stage (60–120 min) was characterized by a slower degradation phase, in which the apparent rate constants of the three treatment technologies (3DES, US, and US-3DES) decreased significantly to 0.001 min^{-1}, 0.002 min^{-1}, and 0.027 min^{-1}, respectively, corresponding to 0.048, 0.2, and 0.692 times those in the first stage. At this stage, most easily degradable substances had already been removed, and the remaining

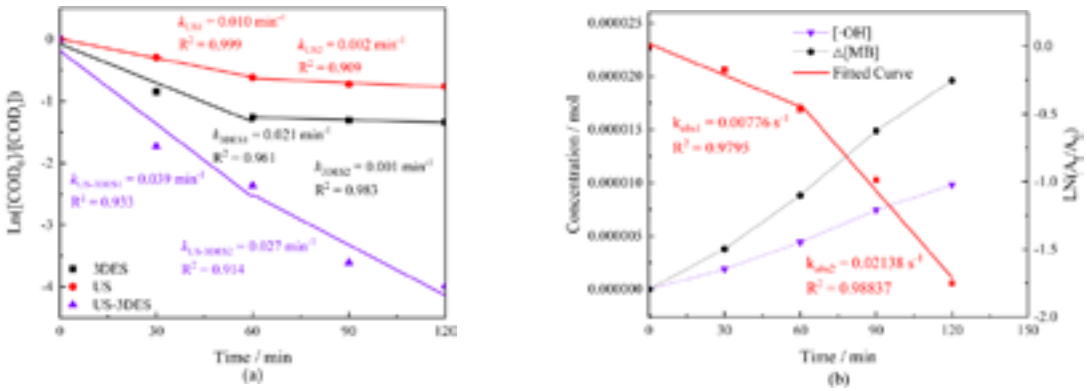

Fig. 8. (a) Reaction kinetics curve fitting; (b) Radical concentration (▼), change in methylene blue (●).

components consisted mainly of refractory macromolecular organics that are difficult to oxidize by free radicals, leading to lower reaction rates. The 3DES system exhibited the lowest rate in this stage, mainly because pollutants and intermediate products accumulated on the electrode surface over time (Li H, et al. 2021), hindering mass transfer. In contrast, the US-3DES system maintained a relatively high degradation rate due to the cavitation-induced shock waves generated by ultrasound, which continuously scour the electrode surface and enhance mass transfer (Barros W R P, et al. 2014). Consequently, the coupled system outperformed the individual processes. According to the synergistic index (SI) [Equation (3); $SI_1 = 1.26$, $SI_2 = 9$], the US-3DES exhibited a significant synergistic effect, with the synergy in the second stage being 7.2 times greater than that in the first stage. This can be explained by the combined effects of enhanced electrochemical mass transfer induced by ultrasound and modulation of the cavitation energy berrier by the electrode potential, leading to increased free radical production. However, Martín de Vidales et al. (2020) reported contrasting results, suggesting an antagonistic effect in ultrasonic-electrochemical systems due to excessive generation and rapid recombination formation and rapid of oxidative free radicals. This discrepancy may be attributed to differences in reactor configuration, as their study employed a two-dimensional electrode system. In contrast, the three-dimensional electrode system used in this study incorporates particle electrodes with porous surfaces, which increase the reaction contact area, improve mass transfer, and promote interactions between free radicals and target pollutants, thereby enhancing overall performance (Zhang, Z, et al. 2024).

Detection of free radical concentration in the US-3DES

A 0.025 mmol·L^{-1} MB solution (1 L) was treated in the US-3DES system under the following conditions: an activated carbon dosage of 60 g, electrode spacing of 5 cm, current density of 50 mA·cm^{-2}, preset voltage of 15 V, and ultrasonic power of 300 W. Samples were taken at 0, 30, 60, 90, and 120 min, and their absorbance was measured at λ = 664 nm using a UV spectrophotometer.

The free radical concentration in the reaction system and the steady-state free radical generation rate were calculated using Equations (7) and (8) [Figure 8(b)]. As the reaction progressed, △[MB] and [·OH] increased, reaching maximum values at 120 min of 1.96×10^{-5} M and 9.8×10^{-6} M, respectively, indicating that free radicals played a dominant role in MB oxidation. However, excessively long reaction times increase both energy consumption (EC) and hydraulic retention time, which in turn require larger reactor volumes and higher capital investment. Therefore, extending the reaction time does not necessarily result in better overall performance. Instead, an optimal reaction time was selected based on cost-effectiveness. Based on the above results, 90 min was determined to be the optimal reaction time.

According to the kinetic equations [Equations (6) and (9)], the steady-state free radical generation rate was calculated to be 9.7×10^{-9} M·s^{-1} in the first reaction stage and 2.67×10^{-8} M·s^{-1} in the second reaction stage. These research results are consistent with those reported in other studies (Lankone R S, et al. 2020, Vo Q V, et al. 2024).In the US-3DES system, the reaction rates of MB and leachate differed between the two stages. For MB, the reaction rate increased in the second stage, likely because the molecules were progressively degraded into smaller, more reactive intermediates. In contrast, leachate

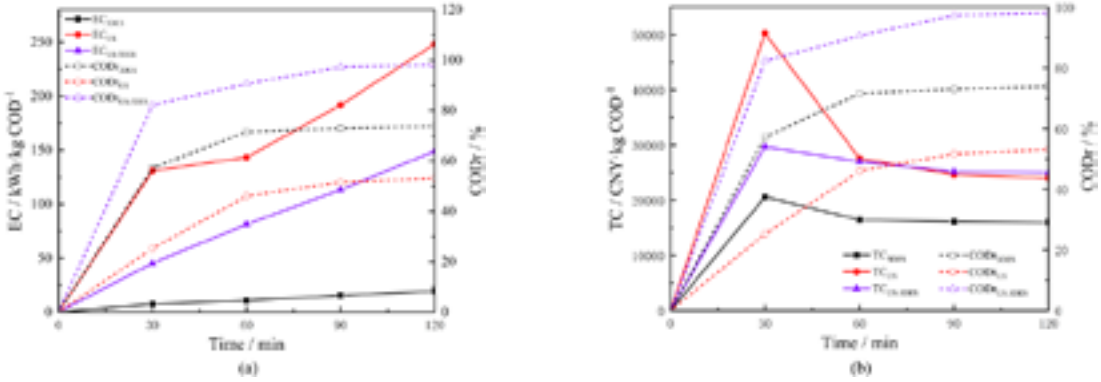

Fig. 9. (a) Comparison of EC and COD removal rate (CODr); (b) Comparison of TC and COD removal rate (CODr).

exhibited a decreased reaction rate in the second stage due to its complex composition. After the readily degradable components were removed in the first stage, the remaining refractory organic matter and intermediate products became more resistant to oxidation, thereby slowing the reaction.

Analysis of EC and TC

The energy consumption of the 3DES system (EC_3DES) was calculated according to Equation (10), while the energy consumption of the US system (EC_US) was determined using the optimal ultrasonic power for COD removal. The energy consumption of the coupled US–3DES system (EC_US–3DES) was calculated based on Equation (11). The comparison of energy consumption with COD removal efficiency is shown in Figure 9(a). The total cost (TC) of the three processes was calculated using Equation (12), and the results are summarized in Table 2. The corresponding comparison with COD removal efficiency is shown in Figure 9(b).

As shown in Figure 9(a), during the reaction process, EC_{US} remained at the highest level, followed by US-3DES, while 3DES exhibited the lowest EC. At a reaction time of 120 min, the EC values of the three reaction systems (3DES, US, and US-3DES) were 19.5 kWh·kg COD^{-1}, 248.2 kWh·kg COD^{-1}, and 149.0 kWh·kg COD^{-1}, respectively. Barros et al. (2014) reported that ultrasonic equipment can significantly increase total EC, which is consistent with the present results. This high EC in the US system is primarily due to its low COD removal efficiency, resulting in greater energy consumption per unit of COD removed. The relatively high $EC_{US\text{-}3DES}$ was mainly contributed by ultrasound; however, its value was lower than the sum of individual US and 3DES systems. This is attributed to the cavitation effect of ultrasound, which enhances mass transfer efficiency and thereby reduces the overall EC of the coupled reaction (Liang S, et al. 2018). Körbahti et al. (2015) reported that a two-dimensional electrode system (2DES) using BDD the electrochemical oxidation of ampicillin had an EC of 71.7 kWh·kg COD^{-1} under optimal operating conditions, which is 3.68 times higher than the EC_{3DES} in the present study. Thus, the 3DES offers significant technical advantages over 2DES in terms of EC.

As shown in Table 2 and Figure 9(b), during the initial stage of the reaction, the treatment cost per unit COD removal was the highest for US system, followed by US-3DES and 3DES, primarily due to the low COD removal efficiency. As the reaction progressed and COD removal increased, the treatment cost per unit of COD removal decreased accordingly. At 120 min, the treatment costs per unit COD removal for the three processes (3DES, US, and US-3DES) were 15,961.6 CNY·kg COD^{-1}, 24,039.7 CNY·kg COD^{-1}, and 25,021.1 CNY·kg COD^{-1}, respectively. The high unit treatment cost l for US system was mainly attributed to the high purchase price of the ultrasonic equipment, which accounted for 99.1% of the total US cost. This also contributed to the elevated unit cost of US-3DES, where the ultrasonic equipment accounting for 51.6% of the total $TC_{US\text{-}3DES}$.

Based on a review of the relevant literature, cost data for other available wastewater treatment processes were compiled in this study, and the results are shown in Table 3.

As indicated in Table 3, the total cost (TC) varied significantly among different wastewater treatment processes. Even for the same treatment method, costs differed depending on wastewater type and treatment scale. Generally, the operating cost of the activated sludge process was much lower than that of various advanced oxidation processes, which partly explains its widespread use in domestic wastewater treatment. However, its efficiency in removing refractory pollutants is limited, highlighting the need for advanced oxidation technologies. Both 3DES and US-3DES demonstrated notable economic advantages, but compared to the former, US-3DES achieved a higher removal efficiency.

Research limitations and future perspectives

This study has several limitations:

(1) Static batch experiments were conducted without considering factors such as hydraulic conditions and reactor design. Therefore, the process parameters cannot be directly applied to continuous-flow systems.

(2) All leachate samples were collected from a single landfill site. Differences in water quality among landfills, landfill age, and seasonal variations were not considered, limiting the generalizability of the findings.

(3) Detailed detection and analysis of intermediate products and active species during the reaction process were not performed. As a result, the reaction mechanisms and degradation pathways of leachate were not fully elucidated. Furthermore, long-term performance and stability studies were not conducted.

To address these limitations, future research will focus

Table 2: Cost analysis of leachate treatment with three reaction systems

	Reaction time / min	Graphite electrode / CNY·L^{-3}	Stainless steel electrode / CNY·L^{-3}	PAC / CNY·kg^{-3}	EC / kWh·kg COD^{-1}	△COD / kg·m^{-3}	TC / CNY·kg COD^{-1}
3DES	120	30	10	12.8	19.5	3.359	15961.6
US		-	-	-	248.2	2.417	24039.7
US-3DES		30	10	12.8	149.0	4.465	25021.1

Notes:

1. The electricity price was calculated at the average industrial electricity price of 0.42 CNY/kWh in Qinghai Province in 2024.
2. The ultrasonic generator was priced at 57,600 CNY, referring to the selling price of ultrasonic cleaning equipment with the required transducer number for 1 m³ of treated water.
3. The DC regulated power supply was calculated at 13,500 CNY per unit for the specification of 0 - 30 V, 100 A.

Table 3: Table 1 The quality of leachate

Treatment technology	Wastewater type	Cost	Remarks
Activated Sludge Process	Domestic wastewater	0.708 CNY·t^{-3}	(Li W, et al. 2017)
		0.22 EUR·m^{-3}	(Molinos-Senante M, et al. 2010)
		0.17~0.87 EUR·m^{-3}	(Santos E, et al. 2022)
High-Rate Algal Pond		0.11–0.87 EUR·m^{-3}	
US-TiO_2	2,4-D herbicide	5071.740 USD·kg COD^{-1}	(Dikmen E, et al. 2022)
US-UV/TiO_2/H_2O_2		4135.229 USD·kg COD^{-1}	
TiO_2/O_3	Oxalic acid	1.51 EUR·m^{-3}	(Mehrjouei M, et al. 2014)
TiO_2/UVA/O_2		13.55 EUR·m^{-3}	
TiO_2/UVA/O_3		3.65 EUR·m^{-3}	
TiO_2/O_3	Dichloroacetic acid	10.75 EUR·m^{-3}	
TiO_2/UVA/O_2		75.35 EUR·m^{-3}	
TiO_2/UVA/O_3		5.16 EUR·m^{-3}	

on three main directions: scaling up the experimental system, analyzing intermediates and active species, and optimizing process performance. The ultimate goal is to advance the application of the US-3DES system from the laboratory scale to broader engineering applications.

Conclusions

In this study, conventional, inexpensive, and unmodified materials were used to evaluate the treatment performance of the US-3DES system for leachate:

(1) With an activated carbon dosage of 60 g, electrode spacing of 5 cm, current density of 50 mA·cm^{-2}, preset voltage of 15 V, and ultrasonic power of 300 W, the COD and UV_{254} removal efficiencies reached maximum values of 82.2% and 96.3%, respectively.

(2) Kinetics analysis revealed that the US-3DES system exhibited two quasi-first-order reaction stages: a rapid reaction stage (0–60 min) and a slow reaction stage (60–120 min).

(3) According to the coupled synergistic index (SI), the ultrasound-three-dimensional electrode coupled reaction system displayed a significant synergistic effect, which was 7.2 times higher in the second stage than in the first stage.

(4) Using methylene blue (MB) as a probe, the concentrations of △[MB] and [·OH] were observed to increase with reaction time, reaching maximum values of 1.96×10^{-5} M and 9.8×10^{-6} M, respectively, at 120 min. The steady-state free radical generation rate was 9.7×10^{-9} M·s^{-1} in the first stage and 2.67×10^{-8} M·s^{-1} in the second reaction stage.

(5) At 120 min, the energy consumption (EC) of the three systems (3DES, US, and US-3DES) was 19.5 kWh·kg COD^{-1}, 248.2 kWh·kg COD^{-1}, and 149.0 kWh·kgCOD^{-1}, respectively. Correspondingly, the total treatment costs (TC) were 15,961.6 CNY·kg COD^{-1}, 24,039.7 CNY·kg COD^{-1}, and 25,021.1 CNY·kg COD^{-1}, respectively.

CRediT author contributions

Xiaoyan Wei: Conceptualization, Methodology, Data curation, Formal analysis, Writing – original draft. **Kang Li:** Conceptualization, Methodology, Writing – original draft. **Wanqi Wang:** Data curation, Writing – original draft. **Tianhong Zhou:** Writing – review & editing. **Jianjun Gao:** Writing – review & editing. **Mingxia Jing:** Data curation. **Shuaiqi Ren:** Data curation. **Fulong Ye:** Data curation. **Hao Wang:** Supervision, Project administration, Final approval of manuscript.

Funding

This work was supported by the Industrial Support Program Project of the Education Department of Gansu Province (Grant No. 2023CYZC-41); the Major Science and Technology Project of Gansu Province (Grant No. 25ZDFA010), and the Lanzhou Urban Water Supply (Group) Scientific Research Project (Grant No. 525113).

Declaration of competing interest

The authors report that there are no competing interests to declare.

Acknowledgements

The authors are sincerely thankful to Qinghai University for providing access to their laboratory facilities. The authors also gratefully acknowledge the Department of Education of Gansu Province, the Department of Science and Technology of Gansu Province, and Lanzhou Urban Water Supply Group Company for their financial support of this research.

References

Abbas S M. & Abas K M. (2025). In situ decoration of Ag@ exfoliated graphite composite catalyst for Fenton-like oxidation of methylene blue dye: kinetic and thermodynamic studies. *BMC chemistry*, 19(1): 221. DOI:10.1186/s13065-025-01584-1.

Ai, Z., Li, J., Zhang, L. & Lee, S. (2010). Rapid decolorization of azo dyes in aqueous solution by an ultrasound-assisted electrocatalytic oxidation process. *Ultrasonics sonochemistry,* 17(2), pp. 370-375. DOI:10.1016/j.ultsonch.2009.10.002.

Arjona, N., Rivas, S., Álvarez-Contreras, L., Guerra-Balcázar, M., Ledesma-García, J., Kjeang, E. & Arriaga, L. G. (2017). Glycerol electro-oxidation in alkaline media using Pt and Pd catalysts electrodeposited on three-dimensional porous carbon electrodes. *New Journal of Chemistry*, 41(4), pp. 1854-1863. DOI:10.1039/C6NJ03739A.

Babuponnusami A. & Muthukumar K. 2012. Advanced oxidation of phenol: a comparison between Fenton, electro-Fenton, sono-electro-Fenton and photo-electro-Fenton processes . *Chemical Engineering Journal*, 183, pp. 1-9. DOI:10.1016/j.cej.2011.12.010.

Barros, W. R., Steter, J. R., Lanza, M. R. & Motheo, A. J. (2014). Degradation of amaranth dye in alkaline medium by ultrasonic cavitation coupled with electrochemical oxidation using a boron-doped diamond anode. *Electrochimica Acta,* 143, pp. 180-187. DOI:10.1016/j.electacta.2014.07.141.

Bodzek M. (2019). Membrane separation techniques -- removal of inorganic and organic admixtures and impurities from water environment -- review. *Archives of Environmental Protection,* 45(4). DOI:10.24425/aep.2019.130237.

Boonphan, S., Prachakiew, S., Klinbumrung, K., Thongrote, C. & Klinbumrung, A. (2024). Enhancing photocatalytic performance of kaolin clay: an overview of treatment strategies and applications. *Archives of Environmental Protection*, 50, 3, pp. 54–64. DOI:10.24425/aep.2024.151686.

Chatraee, M, Ebrahimi A.& Fatehizadeh, A. (2022). Enhanced electro-Fenton processes by persulfate radical for atenolol oxidation from aqueous solution. *Environmental Health Engineering and Management Journal*, 9(2), pp. 147-155. DOI:10.34172/ehem.2022.16.

Cho, S,, Kim, C. & Hwang, I. (2020). Electrochemical degradation of ibuprofen using an activated-carbon-based continuous-flow three-dimensional electrode reactor (3DER). *Chemosphere,* 259, 127382. DOI:10.1016/j.chemosphere.2020.127382.

Dikmen, E., Dogdu, G. & Yalcuk, A. (2022). Comparison Performances of Hybrid Sonocatalysis and Sonophotocatalysis on the Elimination of 2, 4-Dichlorophenoxyacetic Acid in Water: Mineralization and Economic Analysis . *Polish Journal of Environmental Studies*, 31(5). DOI:10.15244/pjoes/149575.

Dionisio, D., Motheo, A. J., Saez, C., Canizares, P. & Rodrigo, M. A. (2019). Coupling ultrasound to the electro-oxidation of methyl paraben synthetic wastewater: effect of frequency and supporting electrolyte . *ChemElectroChem*, 6(4), pp.1199-1205. DOI:10.1002/celc.201801199.

Djeffal, K., Bouranene, S., Fievet, P., Déon, S. & Gheid, A. 2021. Treatment of controlled discharge leachate by coagulation-flocculation: influence of operational conditions. Separation Science and Technology, 56(1), pp. 168-183. DOI:10.1080/01496395.2019.1708114.

Erel, O. (2004). A novel automated method to measure total antioxidant response against potent free radical reactions. *Clinical biochemistry*, 37(2), pp. 112-119. DOI:10.1016/j.clinbiochem.2003.10.014.

Ghjeer, A. Y. & Abbar, A. H. (2023). A comparative study of four technologies (Fenton, Sono-Fenton (SF), Electro-Fenton (EF), and Sono-Electro-Fenton (SEF)) for hospital wastewater treatment . *Case Studies in Chemical and Environmental Engineering*, 8: 100519. DOI:10.1016/j.cscee.2.

Hassani, A., Malhotra, M., Karim, A. V., Krishnan, S. & Nidheesh, P. V. (2022). Recent progress on ultrasound-assisted electrochemical processes: A review on mechanism, reactor strategies, and applications for wastewater treatment. *Environmental Research*, 205, 112463. DOI:10.1016/j.envres.2021.112463.

Hassani, A., Pourshirband, N., Sayyar, Z. & Eghbali, P. (2025). Fenton and Fenton-like-based advanced oxidation processes[M]// Innovative and Hybrid Advanced Oxidation Processes for Water Treatment. Elsevier, pp. 171-203. DOI:10.1016/B978-0-443-14100-3.00006-5.

HBremner, D. E., Burgess, A. & Chand, R. (2011). The chemistry of ultrasonic degradation of organic compounds. *Current Organic Chemistry*, 15(2), pp. 168-177. DOI:10.2174/138527211793979862.

He, Y., Wang, X., Huang, W., Chen, R., Zhang, W., Li, H. & Lin, H. 2018. Hydrophobic networked PbO_2 electrode for electrochemical oxidation of paracetamol drug and degradation mechanism kinetics. *Chemosphere,* 193, pp. 89-99. DOI:10.1016/j.chemosphere.2017.10.144.

Hosseinikhah, M., Ghalebizade, M., Hassani, A., Behzadian, K., Wacławek, S., Lin, K. Y. A. & Ghanbari, F. (2025). An efficient sequential method for enhanced landfill leachate treatment and detoxification: Electrocoagulation/permanganate, peroxymonosulfate-based process, and electro-peroxone. *Journal of Environmental Management*, 388, 125785. DOI:10.1016/j.jenvman.2025.125785.

Huang, Z., Zhao, L., Zhu, J. & He, D. (2024). Three-Dimensional Electrochemical Oxidation System with RuO_2-IrO_2/Ti as the Anode for Ammonia Wastewater Treatment. *Sustainability*, 16(5), 1838. DOI:10.3390/su16051838.

Kanmani, S. & Dileepan, A.G.B. (2023). Treatment of landfill leachate using photocatalytic based advanced oxidation process–a critical review. *Journal of Environmental Management*, 345, 118794. DOI:10.1016/j.jenvman.2023.118794.

Körbahti, B. K. & Taşyürek, S. (2015). Electrochemical oxidation of ampicillin antibiotic at boron-doped diamond electrodes and process optimization using response surface methodology. *Environmental Science and Pollution Research*, 22(5), pp- 3265-3278. DOI:10.1007/s11356-014-3101-7.

Kuchtová, G., Chýlková, J., Váňa, J., Vojs, M. & Dušek, L. (2020). Electro-oxidative decolorization and treatment of model wastewater containing Acid Blue 80 on boron doped diamond and platinum anodes. *Journal of Electroanalytical Chemistry*, 863, 114036. DOI:10.1016/j.jelechem.2020.114036.

Lankone, R. S., Deline, A. R., Barclay, M. & Fairbrother, D. H. (2020). UV–Vis quantification of hydroxyl radical concentration and dose using principal component analysis. *Talanta,* 218, 121148. DOI:10.1016/j.talanta.2020.121148.

Li, M., Zhao, F., Sillanpää, M., Meng, Y. & Yin, D. (2015). Electrochemical degradation of 2-diethylamino-6-methyl-4-hydroxypyrimidine using three-dimensional electrodes reactor with ceramic particle electrodes. *Separation and Purification Technology*, 156, pp. 588-595.

Li, H., Yang, H., Cheng, J., Hu, C., Yang, Z. & Wu, C. (2021). Three-dimensional particle electrode system treatment of organic wastewater: A general review based on patents. *Journal of Cleaner Production,* 308, 127324. DOI:10.1016/j.jclepro.2021.127324.

Li, W., Li, L. & Qiu, G. (2017). Energy consumption and economic cost of typical wastewater treatment systems in Shenzhen, China. *Journal of Cleaner Production*, 163, S374-S378. DOI:10.1016/j.jclepro.2015.12.109.

Liang, S., Lin, H., Yan, X. & Huang, Q. (2018). Electro-oxidation of tetracycline by a Magnéli phase Ti_4O_7 porous anode: Kinetics, products, and toxicity. *Chemical Engineering Journal,* 332, pp. 628-636. DOI:628-636.10.1016/j.cej.2017.09.109.

Liu, J., Wu, H., Sun, J., Li, S., Hassani, A. & Zhou, M. (2025). Non-TiO_2-based photoanodes for photoelectrocatalytic wastewater treatment: electrode synthesis, evaluation, and characterization. *EES Catalysis*. 3(5), pp. 921-942. DOI:10.1039/D5EY00068H.

Ma, J., Wang, X., Sun, H., Tang, W. & Wang, Q. (2023). A review on three-dimensional electrochemical technology for the antibiotic wastewater treatment. *Environmental Science and Pollution Research*, 30(29), pp. 73150-73173. DOI:10.1007/s11356-023-27565-2.

Mehrjouei, M., Müller, S. & Möller, D. (2014). Energy consumption of three different advanced oxidation methods for water treatment: a cost-effectiveness study. *Journal of Cleaner Production*, 65, pp. 178-183. DOI:10.1016/j.jclepro.2013.07.036.

Moholkar, V. S., Sable, S. P. & Pandit, A.B. (2000). Mapping the cavitation intensity in an ultrasonic bath using the acoustic emission. *AIChE Journal*, 46(4), pp. 684-694. DOI:10.1002/aic.690460404.

Molinos-Senante, M., Hernández-Sancho, F. & Sala-Garrido, R. (2010). Economic feasibility study for wastewater treatment: A cost–benefit analysis. *Science of the Total Environment*, 408(20), pp. 4396-4402. DOI:10.1016/j.scitotenv.2010.07.014.

Nalladiyil, A., Prakash, P. & Babu, G.L.S. (2023). Garbage enzyme-mediated treatment of landfill leachate: A sustainable approach. *Bioresource technology,* 385, 129361. DOI:10.1016/j.biortech.2023.129361.

Parthenidis, P., Evgenidou, E. & Lambropoulou, D. (2022). Wet and supercritical oxidation for landfill leachate treatment: a short review. *Journal of Environmental Chemical Engineering*, 10(3), 107837. DOI:10.1016/j.jece.2022.107837.

Periyasamy, S., Lin, X., Ganiyu, S. O., Kamaraj, S. K., Thiam, A. & Liu, D. (2022). Insight into BDD electrochemical oxidation of florfenicol in water: Kinetics, reaction mechanism, and toxicity. *Chemosphere*, 288, 132433. DOI:10.1016/j.chemosphere.2021.132433.

Remmas, N., Manfe, N., Zerva, I., Melidis, P., Raga, R. & Ntougias, S. (2023). A critical review on the microbial ecology of landfill leachate treatment systems . *Sustainability*, 15(2), 949. DOI:10.3390/su15020949.

Ren, X., Fu, H., Peng, D., Shen, M., Tang, P., Song, K., Lai, B. & Pan, Z. (2024). Intensive Treatment of Organic Wastewater by Three-Dimensional Electrode System within Mn-Loaded Steel Slag as Catalytic Particle Electrodes. *Molecules,* 29(5), 952. DOI:10.3390/molecules29050952.

Santos, E., Albuquerque, A., Lisboa, I., Murray, P. & Ermis, H. (2022). Economic assessment of energy consumption in wastewater treatment plants: Applicability of alternative nature-based technologies in Portugal. *Water*, 14(13), 2042. DOI:10.3390/w14132042.

Satoh, A.Y., Trosko, J.E, & Masten, S.J. (2007). Methylene blue dye test for rapid qualitative detection of hydroxyl radicals formed in a Fenton's reaction aqueous solution. *Environmental science & technology*, 41(8), pp. 2881-2887. DOI:10.1021/es0617800.

Shen, B., Wen, X. & Huang, X. (2017). Enhanced removal performance of estriol by a three-dimensional electrode reactor. *Chemical Engineering Journal*, 327, pp. 597-607. DOI:10.1016/j.cej.2017.06.121.

Shi, H., Wang, Q., Ni, J., Xu, Y., Song, N. & Gao, M. (2020). Highly efficient removal of amoxicillin from water by three-dimensional electrode system within granular activated carbon as particle electrode. *Journal of Water Process Engineering*, 38, 101656. DOI:10.1016/j.jwpe.2020.101656.

Sopaj, F., Rodrigo, M.A.,Oturan, N., Podvorica, F.I., Pinson, J. & Oturan, M.A. (2015). Influence of the anode materials on the electrochemical oxidation efficiency. Application to oxidative degradation of the pharmaceutical amoxicillin . *Chemical Engineering Journal*, 262, pp. 286–294. DOI:10.1016/j.cej.2014.09.100.

Testolin, R. C., Mater, L., Radetski-Silva, R., Sanches-Simões, E., Pimentel-Almeida, W., Schmidt, G. T., Ariente-Neto, R., Corrêa, A. X. R., Somensi, C. A. & Radetski, C. M. (2021). Petroleum-contaminated soil: using sonolysis to improve mineralization and biodegradation potential of Fenton reaction and ozonolysis process. *Environmental Science and Pollution Research*, 28(13), pp. 16532-16543. DOI:10.1007/s11356-020-12187-9.

Wang, C., Chen, R., Zhang, R. & Zhang, N. (2018). Simple spectrophotometric determination of sulfate free radicals. *Analytical Methods,* 10(28), pp. 3470-3474. DOI:10.1039/C8AY01194J.

Wei, X., Li, K., Wang, W., Zhou, T., Gao, J., Jing, M., Cao, X., Lu, K., Zhang, G. & Wang, H. (2024). Three-dimensional-electrode Electrochemical Oxidation of Refractory Organic Matter in a Cold High-altitude Area: A Case Study of Dibutyl Phthalate. *Rocznik Ochrona Środowiska,* 26, pp. 356-365. DOI:10.54740/ros.2024.034.

Wu, C., Chen, W., Gu, Z. & Li, Q. 2021. A review of the characteristics of Fenton and ozonation systems in landfill leachate treatment. *Science of the Total Environment*, 762: 143131. DOI:10.1016/j.scitotenv.2020.143131.

Xie, Z., Wang, Z., Wang, Q., Zhu, C. & Wu, Z. 2014. An anaerobic dynamic membrane bioreactor (AnDMBR) for landfill leachate treatment: performance and microbial community identification. *Bioresource technology*, 161, pp. 29-39. DOI:10.1016/j.biortech.2014.03.014.

Yang, W., Li, D., Zhang, J. & Wang, Z. (2022), Removal of ammonia nitrogen from wastewater by three-dimensional electrode system based on solid waste containing iron. *Environmental Engineering Research,* 27(6). DOI:10.4491/eer.2021.411.

Yang, H., Luo, B., Lei, S., Wang, Y., Sun, J., Zhou, Z., Zhang, Y. & Xia, S. (2021). Enhanced humic acid degradation by Fe_3O_4/ultrasound-activated peroxymonosulfate: Synergy index, non-radical effect and mechanism. *Separation and Purification Technology*, 264, 118466. DOI:10.1016/j.seppur.2021.118466.

Yao, Y., Pan, Y. & Liu, S. (2020). Power ultrasound and its applications: A state-of-the-art review. *Ultrasonics sonochemistry*, 62, 104722. DOI:10.1016/j.ultsonch.2019.104722.

Yu, D., Cui, J., Li, X., Zhang, H. & Pei, Y. (2020). Electrochemical treatment of organic pollutants in landfill leachate using a three-dimensional electrode system. *Chemosphere,* 243, 125438. DOI:10.1016/j.chemosphere.2019.125438.

Vo, Q. V., Thao, L. T. T., Manh, T. D., Van Bay, M., Truong-Le, B. T., Hoa, N. T. & Mechler, A. (2024). Reaction of methylene blue with OH radicals in the aqueous environment: mechanism,

kinetics, products and risk assessment. *RSC advances,* 14(37), pp. 27265-27273. DOI:10.1039/d4ra05437g.

Yurchenko, O.I., Chernozhuk, T.V., Kravchenko, O.A. & Baklanov, A. N. (2021). Ultrasound in chemical analysis of mineralized water and brines. *Theoretical & Applied Science* Учредители: Теоретическая и прикладная наука, (10), pp. 680-683. DOI:10.15863/tas.2021.10.102.67.

Zambrano, J., Park, H. & Min, B. (2020). Enhancing electrochemical degradation of phenol at optimum pH condition with a Pt/Ti anode electrode. *Environmental technology*, 41(24), pp. 3248-3259. DOI:10.1080/09593330.2019.1649468.

Zhang, Z., Shen, S., Xu, Q., Cui, L., Qiu, R. & Huang, Z. (2024). Electrochemical oxidation of ammonia in a granular activated carbon/peroxymonosulfate/chlorine three-dimensional electrode system. *Separation and Purification Technology*, 342, 127038. DOI:10.1016/j.seppur.2024.127038.

Zhang, N., Bu, J., Meng, Y., Wan, J., Yuan, L. & Peng, X. (2020). Degradation of p-aminophenol wastewater using Ti-Si-Sn-Sb/GAC particle electrodes in a three-dimensional electrochemical oxidation reactor. *Applied Organometallic Chemistry,* 34(6), e5612. DOI:10.1002/aoc.5612.

Zhang, C., Lin, H., Chen, J. & Zhang, W. 2013. Advanced treatment of biologically pretreated coking wastewater by a bipolar three-dimensional electrode reactor. *Environmental technology*, 34(16), pp. 2371-2376. DOI:10.1080/09593330.2013.770559.

Zhao, H., Gao, J., Zhou, W., Wang, Z. & Wu, S. (2015). Quantitative detection of hydroxyl radicals in Fenton system by UV-vis spectrophotometry. *Analytical Methods*, 7(13), pp. 5447-5453. DOI:10.1039/C5AY00514K.

Zhu, X., Ni, J., Xing, X., Li, H. & Jiang, Y. (2011). Synergies between electrochemical oxidation and activated carbon adsorption in three-dimensional boron-doped diamond anode system. *Electrochimica Acta*, 56(3), pp. 1270-1274. DOI:10.1016/j.electacta.2010.10.073.